

Minimal dynamical symmetry breaking of the standard model

William A. Bardeen, Christopher T. Hill, and Manfred Lindner
Fermi National Accelerator Laboratory, P.O. Box 500, Batavia, Illinois 60510
 (Received 21 July 1989; revised manuscript received 2 November 1989)

We formulate the dynamical symmetry breaking of the standard model by a top-quark condensate in analogy with BCS theory. The low-energy effective Lagrangian is the usual standard model with supplemental relationships connecting masses of the top quark, W boson, and Higgs boson which now appears as a $\bar{t}t$ bound state. Precise predictions for m_t and m_H are obtained by abstracting the compositeness condition for the Higgs boson to boundary conditions on the renormalization-group equations for the full standard model at high energy.

I. INTRODUCTION

The top quark is now known to be more massive than 77 GeV within the context of the standard model. Therefore, its coupling to the elementary Higgs scalar is large, at least of order g_2 , the SU(2) gauge coupling constant at low energies, and possibly larger. Strong coupling suggests that the symmetry breakdown of the standard model may be a dynamical mechanism which intimately involves the top quark, and several authors,^{1,2} most notably Nambu,¹ have recently experimented with this idea. Essentially one implements a BCS or Nambu–Jona-Lasinio mechanism in which a new fundamental interaction associated with a high-energy scale Λ is used to trigger the formation of a low-energy condensate $\langle \bar{t}t \rangle$. The bootstrapping of the symmetry-breaking mechanism to the top quark introduces no fundamental Higgs-scalar bosons and, by virtue of its economy, leads to new predictions which are in principle testable, or which constrain or rule out the mechanism altogether. In particular, we are able to derive predictions for m_t and m_H in this scheme.

This is the minimal conceivable dynamical breaking of the standard model in terms of the relevant number of field degrees of freedom, in which we treat the gauge bosons as fundamental. The usual Cabibbo-Kobayashi-Maskawa structure and fermion mass spectrum is readily accommodated, but *bona fide* predictions of mixing angles and light-quark masses are not derivable until one specifies the dynamics at the scale Λ more precisely. The usual one-Higgs-doublet standard model emerges as the low-energy effective Lagrangian, but with new constraints that lead to nontrivial predictions.

We begin with an analysis of the gauged Nambu–Jona-Lasinio mechanism³ applied to the standard model, within the approximation of keeping only the effects of the fermionic determinant as described below. This yields the “bare” mass relationship, but the most important new results which emerge are the compositeness conditions pertaining to the Higgs-boson bound state, with an otherwise conventional low-energy effective Lagrangian for the standard model. We translate these conditions into boundary conditions at the scale Λ on the renormalization-group equations for the

full theory, which now includes the effects of gauge-boson and Higgs-boson loops, etc. Certain renormalization-group trajectories are thereby associated with the existence of composite structure. These lead to precise predictions for m_t and m_H , which are very insensitive to the scale of new physics Λ .

We show that the compositeness condition is the statement that the induced wave-function renormalization constant Z_H for the Higgs field H must vanish at the scale Λ (see related earlier works as in Ref. 4). It is just this condition, coupled to our demand for a symmetry-breaking solution to the theory at low energies, which enables one to “predict” the mass of the top quark and the mass of the dynamical scalar Higgs boson. The composite theory is effectively a strongly coupled (Higgs-Yukawa and quartic Higgs-boson couplings) standard model near the scale Λ . The low-energy predictions that emerge are governed by infrared renormalization-group fixed points.⁵ The top quark is predicted to lie near 230 GeV for $\Lambda \sim 10^{15}$ GeV. We discuss in some detail the consistency of these predictions with the collection of experimental results that constitute the so-called ρ parameter bound, and we conclude that *it is premature to rule out top-quark masses as high as ~ 250 GeV.*

Our preliminary goal is to make precise the definition of the minimal dynamical-symmetry-breaking scheme beginning with a well-defined quantum field theory at the scale Λ . We imagine that at some high-energy scale Λ the standard model contains only the usual quark, lepton, and gauge-boson degrees of freedom, but no fundamental Higgs scalar. We then introduce a new effective four-fermion vertex with a coefficient G of order $1/\Lambda^2$. This interaction must, of course, be fully gauge invariant. If we consider, for discussion, the approximation in which all quarks and leptons other than the top quark are massless we may then define the theory at the scale Λ to be

$$L = L_{\text{kinetic}} + G(\bar{\Psi}_L^{ia} t_{Ra})(\bar{t}_R^b \Psi_{Lib}), \quad (1.1)$$

where i runs over SU(2)_L indices, (a, b) run over color indices, and L_{kinetic} contains the usual gauge-invariant fermion and gauge-boson kinetic terms, but there is no Higgs field in L . The model readily generalizes to a more realistic mass spectrum, as well as a multiple effective Higgs-doublet scheme as described below in Sec. III.

We first consider a solution based upon the effects of the fermionic determinant alone, i.e., a fermion bubble approximation. This is equivalent to a large- N_{color} expansion in the limit in which the QCD coupling constant is set to zero, and it captures nonperturbative features of the theory from the point of view of a small-coupling-constant expansion. We demand a self-consistent dynamical solution to the gap equation for the mass of the top quark, given in terms of an induced vacuum matrix element of the form $\langle \bar{t}t \rangle$. This will generate poles in the scalar and pseudoscalar channels, corresponding to a physical state with a mass of $2m_t$ and zero-mass Goldstone bosons, respectively. From the vector-boson vacuum-polarization analysis we determine the electroweak vector-boson masses in terms of the top-quark mass. Moreover, we will see that the low-energy-induced Lagrangian has all of the renormalization properties, and is indistinguishable from, the standard model with a single Higgs doublet. The essential results of this analysis are presented in Sec. II, while the full technical details are given in Appendixes A and B.

The central result is that the physical Higgs boson is composite and both the top-quark and Higgs-boson masses become related to the observable electroweak scale. Here we do not address the usual problem of the gauge hierarchy, i.e., how we can naturally maintain the hierarchy of scales $M_W \ll \Lambda$. It should be noted, however, that the quadratic divergence fine-tuning problem is isolated in the gap equation sector of this analysis; once the gap equation is satisfied for a symmetry-breaking scale of order M_W , there is no further fine-tuning needed.

We emphasize that the predictions of the fermionic determinant analysis are inherently limited. The discussion of this approximation will be presented in Sec. II, but we emphasize that it is intended only as a schematic for the full theory, i.e., the fermionic determinant analysis should be viewed only as a model discussion of the actual physical situation. It neglects, e.g., radiative corrections due to gauge bosons and propagation of the composite Higgs boson itself. It is only upon abstracting the compositeness conditions to the full theory that we obtain reliable predictions for m_t and m_H .

Thus we begin in Sec. II with a digest of the fermionic determinant analysis, with the full technical details given in Appendixes A and B. In Sec. III we write the effective Lagrangian in terms of the induced low-energy composite particles. In Sec. IV we present the analysis of the full theory and give precise results that include all of the effects in the standard model. We discuss the viability of the results in light of the most stringent limits on m_t from the “ ρ parameter” analysis in Sec. IV B. In Sec. V we present our conclusions and compare our results to other recent works.

II. FERMIONIC DETERMINANT APPROXIMATION

The present discussion summarizes how the dynamical-symmetry-breaking mechanism through top-quark condensation works in the approximation of keeping only fermionic loops, or, equivalently, to leading order in $1/N_c$ with the QCD coupling constant set to zero.

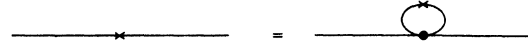


FIG. 1. Diagrammatic representation of the gap equation.

This section is mostly a digest of results, and a more detailed discussion is given in Appendixes A and B. We presently ignore all gauge-boson and composite-Higgs-boson radiative corrections. The “bare” relationships emerge between the composite-Higgs-boson, top-quark, and W -boson masses. These relationships are only approximate, and in Sec. IV we will give the precise predictions, after abstracting the compositeness conditions to the full theory.

A. Gap equation

We will begin by summing the planar bubble diagrams in which the four-fermion interaction of Eq. (1.1) is iterated. We first consider the solution to the gap equation for the induced top-quark mass. This is indicated as in Fig. 1:

$$m_t = -\frac{1}{2}G\langle \bar{t}t \rangle \quad (2.1)$$

$$= 2GN_c m_t \frac{i}{(2\pi)^4} \int d^4l (l^2 - m_t^2)^{-1}. \quad (2.2)$$

The result of evaluating Eq. (2.2) with a momentum-space cutoff Λ is

$$G^{-1} = \frac{N_c}{8\pi^2} [\Lambda^2 - m_t^2 \ln(\Lambda^2/m_t^2)], \quad (2.3)$$

which has solutions for sufficiently strong coupling, $G \geq G_c = 8\pi^2/N_c \Lambda^2$ where G_c is the “critical” coupling constant.

Here, we regard G and Λ as fundamental parameters of the theory and we solve for m_t . Normally, for very large Λ , perhaps of the order of the grand-unified-theory (GUT) scale 10^{15} GeV, we would expect the solution of this equation to produce a large mass, $m_t \sim \Lambda$ in the broken-symmetry phase. We see that a solution for $m_t \sim M_W$ for such large Λ constitutes a fine-tuning problem in that $G^{-1} - G_c^{-1}$ must then be very small. This is, indeed, the usual fine-tuning or gauge-hierarchy problem of the standard model. The gap equation contains a quadratic divergence, corresponding to the usual Higgs-boson mass quadratic divergence in the standard model. However, the fine-tuning problem will be isolated in the gap equation; i.e., once we tune G to admit the desirable solution we need cancel no other quadratic divergences in other amplitudes.

B. Scalar and Goldstone modes

Let us now assume that the parameters G , Λ admit a solution for m_t to the gap equation, Eq. (2.3). We now consider the sum of scalar channel fermion bubbles of Fig. 2 generated by the interaction Eq. (1.1):

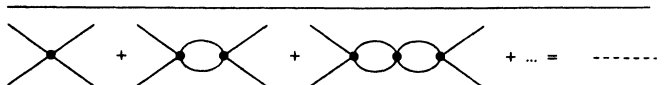


FIG. 2. Bubble sum generated by the four-fermion interaction.

$$\Gamma_s(p^2) = -\frac{1}{2}G - (\frac{1}{2}G)^2 i \int d^4x e^{ipx} \langle T \bar{t}(0) \bar{t}(x) \rangle_{\text{connected}} + \dots \quad (2.4)$$

A useful technical trick for evaluating this amplitude while simultaneously implementing the gap equation is given in Appendix A. The result is

$$\Gamma_s(p^2) = \frac{1}{2N_c} \left\{ (p^2 - 4m_t^2)(4\pi)^{-2} \times \int_0^1 dx \ln \{ \Lambda^2 / [m_t^2 - x(1-x)p^2] \} \right\}^{-1} \quad (2.5)$$

Γ_s is the propagator for the dynamically generated bound state, a scalar composite of $\bar{t}t$. In particular, owing to the pole at $p^2 = 4m_t^2$, we see that the theory predicts a scalar bound state with a mass of $2m_t$ (Ref. 1). This is a standard result quoted for the Nambu–Jona-Lasinio model. We emphasize that this bound state is the physical, observable, low-energy Higgs boson, and the prediction holds here only to leading order in $1/N_c$ in the absence of gauge-boson corrections.

This physical particle is a bound state of $\bar{t}t$, arising by the attractive four-fermion interaction at the scale Λ of Eq. (1.1). One might think that this is a loosely bound state, since it lies on top of the threshold for open $\bar{t}t$ and apparently has vanishing binding energy to this order. However, this is *not a nonrelativistic bound state*, and normal intuition does not apply. The prediction $m_H = 2m_t$ cannot be viewed at this stage as a very precise one. In fact, the essential point is only that this is a composite-Higgs-boson model and we will give a more

precise determination of its mass in Sec. IV upon considering the full renormalization-group behavior of the complete theory.

Since the mechanism is a dynamical breaking of the continuous $SU(2) \times U(1)$ symmetry, it must imply the existence of Goldstone modes. Moreover, the symmetry breaking transforms as $I = \frac{1}{2}$ and will produce the same spectrum of Goldstone bosons as in the standard-model Higgs sector. A Goldstone pole thus appears in the bubble sum for the neutral-pseudoscalar channel:

$$\Gamma_p(p^2) = -\frac{1}{2}G - (\frac{1}{2}G)^2 i \times \int d^4x e^{ipx} \langle T \bar{\gamma}_5 t(0) \bar{\gamma}_5 t(x) \rangle_{\text{connected}} + \dots \quad (2.6)$$

By similar manipulations as in Eq. (2.5) and use of the gap equation we find

$$\Gamma_p(p^2) = \frac{1}{2N_c} \left\{ (p^2)(4\pi)^{-2} \times \int_0^1 dx \ln \{ \Lambda^2 / [m_t^2 - x(1-x)p^2] \} \right\}^{-1} \quad (2.7)$$

and the Goldstone pole at $p^2 = 0$ is seen to occur explicitly.

Moreover, charged Goldstone modes appear in the flavored channels corresponding to the quantum numbers of the W boson:

$$\Gamma_F = -\frac{1}{4}G - (\frac{1}{4}G)^2 i \int d^4x e^{ipx} \langle T \bar{b}(1 + \gamma_5) t(0) \bar{t}(1 - \gamma_5) b(x) \rangle_{\text{connected}} + \dots \quad (2.8)$$

whence

$$\Gamma_F(p^2) = \frac{1}{8N_c} \left\{ (p^2)(4\pi)^{-2} \int_0^1 dx (1-x) \ln \{ \Lambda^2 / [(1-x)m_t^2 - x(1-x)p^2] \} \right\}^{-1} \quad (2.9)$$

where we have assumed $m_b \approx 0$.

C. Vector bosons

Thus far we have considered only a conventional Nambu–Jona-Lasinio model for the symmetry group $SU(2) \times U(1)$ in the absence of gauge fields. Now let us consider the model with the gauge coupling constants restored. Of course, we have a dynamical Higgs mechanism and the gauge bosons acquire masses by “absorbing” the dynamically generated Goldstone poles. We obtain a second prediction of the theory in the form of a relation between the W -boson mass and the top-quark mass.

Consider now the inverse propagator of the gauge bosons. We rescale fields to bring the gauge coupling constants into the gauge-boson kinetic terms; i.e., we write the kinetic terms in the form $(-1/4g^2)(F_{\mu\nu})^2$. We are

not integrating over the gauge-boson fields and need specify no gauge fixing at this stage. Thus, for the W boson we have

$$\frac{1}{g_2^2} D_{\mu\nu}^W(p)^{-1} = \frac{1}{g_2^2} (p_\mu p_\nu - g_{\mu\nu} p^2) + \frac{i}{2} \int d^4x \langle T \bar{t}_L \gamma_\mu b_L(0) \bar{b}_L \gamma_\nu t_L(x) \rangle \quad (2.10)$$

where g_2 is the $SU(2)$ coupling constant. For the T -ordered product we again expand in the interaction Lagrangian of Eq. (1.1) and sum the planar bubbles, Fig. 3.



FIG. 3. The planar loops contributing to gauge-boson propagators.

We assume the top quark has a mass satisfying Eq. (2.3), and the gap equation is satisfied in the loop expansion, which maintains the gauge invariance. This sum can thus be written in terms of the flavor bubbles evaluated in Eq. (2.9) (see Appendix A).

It is useful to write the induced inverse W -boson propagator in the form

$$\frac{1}{g_2^2} D_{\mu\nu}^W(p)^{-1} = (p_\mu p_\nu / p^2 - g_{\mu\nu}) \left[\frac{1}{\bar{g}_2^2(p^2)} p^2 - \bar{f}^2(p^2) \right]. \quad (2.11)$$

The W -boson mass is the solution to the mass-shell condition

$$M_W^2 = p^2 = \bar{g}_2^2(p^2) \bar{f}^2(p^2), \quad (2.12)$$

while the Fermi constant is the zero-momentum expression

$$\frac{G_F}{\sqrt{2}} = \frac{1}{8\bar{f}^2(0)}. \quad (2.13)$$

Note, therefore, that our normalization conventions relate $\bar{f}(0)$ to the standard-model Higgs vacuum expectation value (VEV) v as follows: $v = (G_F \sqrt{2})^{-1/2} = 246$ GeV $= 2\bar{f}(0)$. In the bubble approximation we find

$$\begin{aligned} \frac{1}{\bar{g}_2^2(p^2)} &= \frac{1}{g_2^2} + N_c (4\pi)^{-2} \int_0^1 dx \, 2x(1-x) \\ &\quad \times \ln \{ \Lambda^2 / [x m_b^2 + (1-x) m_t^2 - x(1-x) p^2] \} \end{aligned} \quad (2.14)$$

and

$$\begin{aligned} \bar{f}^2(p^2) &= N_c (4\pi)^{-2} \int_0^1 dx \, [x m_b^2 + (1-x) m_t^2] \\ &\quad \times \ln \{ \Lambda^2 / [x m_b^2 + (1-x) m_t^2 - x(1-x) p^2] \}. \end{aligned} \quad (2.15)$$

At this stage of the approximation it is useful to note the quantitative result for m_t in terms of G_F . Equation (2.13) combined with Eq. (2.15) gives

$$\begin{aligned} \bar{f}^2(0) &= \frac{1}{4\sqrt{2}G_F} \\ &\approx N_c (4\pi)^{-2} \int_0^1 (1-x) m_t^2 \ln \{ \Lambda^2 / [(1-x) m_t^2] \} \\ &\approx \frac{1}{2} N_c (4\pi)^{-2} m_t^2 \ln(\Lambda^2 / m_t^2). \end{aligned} \quad (2.16)$$

For example, with $\Lambda = 10^{15}$ GeV one finds $m_t \approx 165$ GeV.

To what extent is this an accurate prediction for m_t ? For one, it is valid only in leading order of $1/N_c$ with $g_3 = 0$. This result, moreover, neglects the full dynamical effects of gauge bosons and the composite Higgs boson, which should be included in the renormalization-group running below the scale Λ . We note that this result is substantially less than our full standard-model result as obtained in Sec. IV.

Analogous results are obtained for the neutral gauge-boson masses, but they contain no additional information beyond that described here, a consequence of the conventional $I = \frac{1}{2}$ breaking mode. The only technical challenge in the analysis is that we now have the mixing between the U(1) and neutral SU(2) gauge bosons induced by the difference between the top-quark and b -quark masses. We give the full analysis of this in Appendix A. Moreover, the usual ρ parameter relationship for m_t is obtained.

In Appendix B we observe that the evolution of the coupling constants g_1 and g_2 [as seen in Eq. (2.14)] is equivalent to that given by the renormalization group for the truncated model in the bubble approximation (i.e., without gauge coupling constants). Thus, the effective Lagrangian at scales below Λ must produce this evolution. We thus turn now to a discussion of this effective Lagrangian.

III. LOW-ENERGY EFFECTIVE LAGRANGIAN

A. Induced Higgs scalar

In Sec. II and Appendixes A and B we derived the low-energy effects of dynamical symmetry breaking provided by a sufficiently attractive four-fermion interaction involving the top quark as defined in Eq. (1.1). We considered a model based on a conventional sum of the fermion bubble diagrams associated with the leading large- N_c limit with $g_3 = 0$. This simple model generates dynamical masses for the top quark and gauge bosons of the standard model, as well as a bound state corresponding to the usual physical Higgs scalar of mass $2m_t$. In Appendix B we show that the fermion bubbles yield their conventional contribution to the running of the gauge coupling constants and the explicit cutoff dependence can be absorbed by appropriate renormalization of these couplings. The effective Higgs vacuum expectation value, $\propto \bar{f}(0)$, has the normal isospin structure related to the ρ parameter but remains sensitive to the cutoff Λ as its dependence cannot be absorbed by renormalization. Our calculations imply that the effective low-energy dynamics is, in fact, just the usual standard model with certain constraints on the fundamental parameters of the theory.

We can see the connection with the standard model by using a Yukawa form of the four-fermion interactions as defined at the cutoff scale Λ , through the help of a static, auxiliary Higgs field H (see, e.g., Eguchi⁴). We can rewrite Eq. (1.1) as

$$L = L_{\text{kinetic}} + g_{t0} (\bar{\Psi}_L t_R H + \text{H.c.}) - m_0^2 H^\dagger H. \quad (3.1)$$

If we integrate out the field H we produce the four-fermion vertex as an induced interaction with $G = g_{t0}^2 / m_0^2$. Note here that $m_0^2 \sim \Lambda^2$, and positive, implies an attractive interaction. For low-energy phenomena we may wish to keep the effective Higgs field and integrate out the short-distance components of the fermion fields. The analysis of Sec. II may be interpreted as implying that at scales below the cutoff Λ Higgs field H develops induced, fully gauge-invariant, kinetic terms and quartic interaction contributions in the effective action.

Indeed, we can exactly reproduce the results of the previous section if use the large- N_c limit to compute the fermion loop contributions.

The full induced effective Lagrangian will take the form

$$L = L_{\text{kinetic}} + g_{t0}(\bar{\Psi}_L t_R H + \text{H.c.}) + \Delta L_{\text{gauge}} + Z_H |D_\mu H|^2 - m_H^2 H^\dagger H - \frac{\lambda_0}{2} (H^\dagger H)^2, \quad (3.2)$$

where D_μ is the gauge-covariant derivative and all loops are now to be defined with respect to a low-energy scale μ . Here ΔL_{gauge} is the usual fermion loop contribution to the renormalization of the gauge coupling constants as given in Sec. IIC and Appendix B. A direct evaluation of the induced parameters in the Lagrangian gives

$$\begin{aligned} Z_H &= (4\pi)^{-2} g_{t0}^2 N_c \ln(\Lambda^2/\mu^2), \\ m_H^2 &= m_0^2 - (4\pi)^{-2} g_{t0}^2 (2N_c)(\Lambda^2 - \mu^2), \\ \lambda_0 &= (4\pi)^{-2} g_{t0}^4 (2N_c) \ln(\Lambda^2/\mu^2). \end{aligned} \quad (3.3)$$

The Lagrangian of Eq. (3.2) is exactly the same as the usual low-energy standard model, except that we are not free to renormalize the two induced parameters Z_H and λ_0 , which must have an explicit dependence upon Λ , vanishing when $\mu \rightarrow \Lambda$. The mechanism for spontaneous symmetry breaking is now seen in the effective Higgs-boson mass which is driven by the additive quadratic dependence upon Λ to a finite, negative value by the fermion loop contributions; the bare mass m_0^2 requires the usual fine-tuning to produce a finite VEV of the Higgs field (or top-quark mass).

We may use the above tree Lagrangian to estimate the physical spectrum of the low-energy theory. First, we rescale the field $H \rightarrow H/\sqrt{Z_H}$ in Eq. (3.2) and then denote the real, physical neutral component of H as $H^0 = h^0/\sqrt{2}$. We then find

$$\begin{aligned} m_t &= g_{t0} \langle h^0 \rangle / \sqrt{2Z_H}, \\ m_{h^0}^2 &= -2m_H^2/Z_H = \lambda_0 \langle h^0 \rangle^2 / Z_H^2 \\ &= 2(\lambda_0/Z_H g_{t0}^2) m_t^2 = 4m_t^2, \\ f^2 &= m_Z^2 / (g_1^2 + g_2^2) = \frac{1}{2} Z_H \langle h^0 \rangle^2 = \frac{1}{2} (Z_H/g_t^2) m_t^2 \\ &= (N_c/2)(4\pi)^{-2} m_t^2 \ln(\Lambda^2/\mu^2) = \bar{f}^2, \end{aligned} \quad (3.4)$$

which agree with the previous results for the divergent parts in Sec. II. Indeed, we have previously noted that the running of the gauge coupling constants are as expected in the leading- N_c approximation. Full agreement with the previous section's results can be achieved by adding the low-energy fermion loop corrections to the results of Eq. (3.4).

At this point it is useful to anticipate the discussion of Sec. IV concerning the renormalization-group evolution of the quartic Higgs-boson coupling constant. The high-energy renormalization-group running of the Higgs quar-

tic coupling λ_0 , as seen in Eq. (3.3) is consistent with the contribution of a single quark-doublet contribution to the renormalization-group equation. The conventional Higgs and Higgs-Yukawa coupling constants should be identified with

$$\lambda = \lambda_0/Z_H^2, \quad g_t = g_{t0}/\sqrt{Z_H}. \quad (3.5)$$

λ satisfies, in the full standard model, the one-loop renormalization-group equation

$$16\pi^2 \frac{\partial}{\partial \ln \mu} \lambda = (12\lambda^2 + 4N_c \lambda g_t^2 - 4N_c g_t^4), \quad (3.6)$$

where the fermion loops contribute the last two terms. Combining Eq. (3.3) for Z_H and λ_0 , with Eq. (3.5) and performing the differentiation with respect to $\ln \mu$, one sees that λ satisfies the renormalization-group equations with only fermion loop effects.

We have seen that the introduction of the four-fermion terms at the scale Λ can be written in terms of the static Higgs field with Yukawa couplings to the fermions. In the large- N_c limit the theory evolves at low energy to a complete standard model with a dynamical Higgs field. The appropriate renormalization-group equations are just those obtained in the usual standard model. The compositeness conditions $Z_H = \lambda_0 = 0$ are associated with the boundary conditions for the running coupling constants at the high-energy scale Λ . The composite Higgs theory can be identified with entire renormalization-group trajectories of the full standard model. This statement is exact in the large- N_c limit as we have shown by explicit calculation.

We now conjecture that this same identification can be made beyond this approximation. At low energy the standard model is not dominated by the fermion loop contributions, and radiative corrections from virtual gauge and Higgs propagation are essential. However, we expect that the renormalization-group trajectories for the composite Higgs theory should be associated with the vanishing of Z_H and λ_0 for the full theory just as the normal Landau ghost poles are associated with the existence of composite gauge bosons. Our treatment of the full renormalization-group equations is given in Sec. IV.

B. Generalizations

The dynamical model presented here may be generalized in several directions. First, it is readily seen that the full standard-model couplings for fermions, including light quarks and leptons, may be incorporated into the structure of the four-fermion Lagrangian. The Yukawa couplings in Eq. (3.1) may be generalized to the full set of massive fermions:

$$\begin{aligned} L &= L_{\text{kinetic}} + g_{ij}^{\text{up}} (\bar{\Psi}_L^i \text{quark} q_R^{j(+2/3)} H + \text{H.c.}) \\ &\quad + g_{ij}^{\text{down}} (\bar{\Psi}_L^i \text{quark} q_R^{j(-1/3)} H^c + \text{H.c.}) \\ &\quad + g_{ij}^{\text{lepton}} (\bar{\Psi}_L^i \text{lepton} q_R^{j(-1)} H^c + \text{H.c.}) - m_0^2 H^\dagger H, \end{aligned} \quad (3.7)$$

where $H_i^c = \epsilon_{ij} H^{j\dagger}$. The standard Cabibbo-Kobayashi-Maskawa structure can be readily input. Also, axion and familon degrees of freedom can occur at the generalized

level of Eq. (3.7). Integrating out the static auxiliary Higgs field produces the fundamental four-fermion interaction.

More general four-fermion interactions may require more than one auxiliary Higgs field which then may also become dynamical at low energies. However, while we can always introduce elementary spectator Higgs doublets into the standard model which do not couple to quarks or leptons, all of the composite Higgs bosons must couple to matter fields. Thus, the dynamical mechanism is less general than the standard model; i.e., the four-fermion interactions admit a limited number of "square roots." An analysis of the allowed dynamical Higgs bosons will be given elsewhere.

The fermion mass matrices observed at low energy depend upon the specific structure of the four-fermion interactions introduced at high energy, and no obvious simplification occurs from the composite Higgs mechanism. We will return to these issues elsewhere.

IV. PREDICTIONS OF THE FULL STANDARD MODEL

A. Renormalization-group boundary conditions

We have seen in Sec. III that the interaction of Eq. (1.1) can be described by an induced auxiliary Higgs scalar. Below the scale Λ the field H acquires gauge-invariant kinetic terms and quartic interactions. The dynamical origin of the Higgs field thus implies special boundary conditions on the Higgs-Yukawa and Higgs-quartic coupling constants at the Higgs compositeness scale Λ .

Consider again the Lagrangian of Eq. (3.2):

$$L = L_{\text{kinetic}} + g_{t0}(\bar{\Psi}_L t_R H + \text{H.c.}) + Z_H |D_\mu H|^2 - m_H^2 H^\dagger H - \frac{\lambda_0}{2} (H^\dagger H)^2. \quad (4.1)$$

We include here the gauge-invariant kinetic terms of the Higgs doublet and its quartic interaction as well as the wave-function normalization constant Z_H and the top quark will have its own gauge-invariant kinetic terms separately for left- and right-handed fields with wave-function normalization constants Z_{tL} and Z_{tR} .

Conventionally one normalizes the kinetic terms of a field theory at any scale μ with a condition that the kinetic terms have free-field theory normalization. That is, we may exercise our freedom of rescaling the various fields, H , Ψ_L , t_R , etc., to define $Z_H = 1$ and $Z_{tL} = Z_{tR} = 1$, etc. This is accomplished by, e.g., computing one-particle-irreducible (1PI) matrix elements of the kinetic terms treated as local operators and obtaining perturbative expressions for the Z_i , and then absorbing these overall multiplicative factors into the fields, $H \rightarrow H/\sqrt{Z_H}$, $\Psi_L \rightarrow \Psi_L\sqrt{Z_{tL}}$, $t_R \rightarrow t_R/\sqrt{Z_{tR}}$, etc. The coupling constants, such as \bar{g}_i and $\bar{\lambda}$ are then renormalized as usual:

$$\bar{g}_i = \frac{Z_{HY}}{\sqrt{Z_H Z_{tL} Z_{tR}}} g_{i0}, \quad \bar{\lambda} = \frac{Z_{4H}}{Z_H^2} \lambda_0, \quad (4.2)$$

where $Z_{HY}(Z_{4H})$ is the proper vertex renormalization

constant for the Higgs-Yukawa (Higgs-quartic) interactions, and the overbar will henceforth denote quantities in the conventional normalization conditions.

In the present case, however, the Higgs field is dynamical with a vanishing wave-function renormalization constant at the scale Λ . It is useful, therefore, to adopt an "unconventional" normalization convention which does not set $Z_H = 1$. At the scale Λ we have a finite coupling constant $G = g_{t0}^2/m_H^2$. That is, we have the following conditions at Λ (in terms of the unconventional normalization):

$$g_{t0} \rightarrow \text{const}, \quad Z_H \rightarrow 0, \quad \lambda_0 \rightarrow 0. \quad (4.3)$$

It is easy to see that the transformation $H \rightarrow H/\bar{g}_i(\mu^2)$ with the running Higgs-Yukawa coupling $\bar{g}_i(\mu^2)$ transforms the conventional normalization into that required by Eq. (4.3). We thus have

$$\tilde{Z}_H = \frac{1}{\bar{g}_i^2(\mu^2)}, \quad (4.4)$$

$$\tilde{\lambda} = \frac{\bar{\lambda}(\mu^2)}{\bar{g}_i^4(\mu^2)}, \quad (4.5)$$

where the tilde will henceforth denote the normalization convention appropriate for compositeness.

The conditions Eqs. (4.4) and (4.5) allow us to discuss the compositeness conditions Eq. (4.3) in terms of the usual running couplings $\bar{g}_i(\mu^2)$ and $\bar{\lambda}(\mu^2)$ of the standard model. It is clear that $\tilde{Z}_H \rightarrow 0$ requires $\bar{g}_i(\mu^2)$ to blow up at Λ . We may utilize the full one-loop β functions (neglecting light-quark masses and mixings) of the standard model:

$$16\pi^2 \frac{d\bar{g}_i}{dt} = \left(\frac{9}{2}\bar{g}_i^2 - 8\bar{g}_3^2 - \frac{9}{4}\bar{g}_2^2 - \frac{17}{12}\bar{g}_1^2\right)\bar{g}_i \quad (4.6)$$

and, for the gauge couplings,

$$16\pi^2 \frac{d\bar{g}_i}{dt} = -c_i \bar{g}_i^3 \quad (4.7)$$

with

$$c_1 = -\frac{1}{6} - \frac{20}{9}N_g, \quad c_2 = \frac{43}{6} - \frac{4}{3}N_g, \quad c_3 = 11 - \frac{4}{3}N_g, \quad (4.8)$$

where N_g is the number of generations and $t = \ln\mu$.

One can see from Eq. (4.6) that once \bar{g}_i is sufficiently large, it will diverge as it evolves to a higher scale. Neglecting the small gauge contributions for sufficiently large \bar{g}_i we have

$$16\pi^2 \frac{d\bar{g}_i}{dt} = \frac{9}{2}\bar{g}_i^3,$$

equivalently,

$$\frac{d\tilde{Z}_H}{dt} = -\frac{9}{16\pi^2} = \text{const} < 0.$$

\tilde{Z}_H thus decreases asymptotically with a linear slope in $t = \ln\mu$ and becomes zero at the Landau singularity of $\bar{g}_i(\mu^2)$ at Λ . Although one-loop β functions do not permit an extrapolation all the way to $\tilde{Z}_H = 0$, a large part of the linear decrease toward the compositeness scale is fully reliable (e.g., $\tilde{Z}_H \gtrsim 0.08$ is within the perturbative regime

of $\bar{\alpha}_t \lesssim 1$). Indeed, lattice gauge theory has generally confirmed that perturbation theory is quantitatively reliable in analyzing the initial conditions leading to these fixed points.⁶ This behavior is illustrated by the solid lines of Fig. 4 where the full Eqs. (4.6) and (4.7) are used to numerically plot \tilde{Z} .

The precise value of the top-quark mass will be given by running $\bar{g}_t(\mu^2)$ from very high values at a given compositeness scale Λ down to the mass-shell condition $\bar{g}_t(m_t^2)v/\sqrt{2}=m_t$. For large \bar{g}_t , the β function Eq. (4.6) is positive and changes slope drastically with changes in \bar{g}_t . Large initial values for \bar{g}_t at Λ become small if one goes to smaller scales and the nonlinearity focuses a wide range of initial values into a small range of final low-energy results. Once \bar{g}_t becomes smaller, the slowly changing gauge couplings are important. For an estimate one can assume that the gauge couplings are constant which indicates why the solutions are attracted toward the “effective low-energy fixed point”:⁵

$$\bar{g}_t^2(\mu^2) \approx \frac{16}{9} \bar{g}_3^2(\mu^2). \quad (4.10)$$

In general, the couplings are only evolved over a finite range of t and the effective fixed point will not always be reached for all initial values. However, for the case of the composite Higgs bosons, as discussed here, the fixed-point is always reached. The action of the effective fixed point makes the top-quark-mass prediction very insensitive to the initial high values of the coupling constant close to Λ . Considering $\tilde{Z}_H \rightarrow 0$, the uncertainties of higher orders can be viewed as an uncertainty in the precise position of Λ [see Fig. (4)].

In Table I we give the resulting physical m_t obtained by a numerical solution of the renormalization-group equations as a function of Λ . We use $M_Z=91.17$ GeV and the gauge couplings

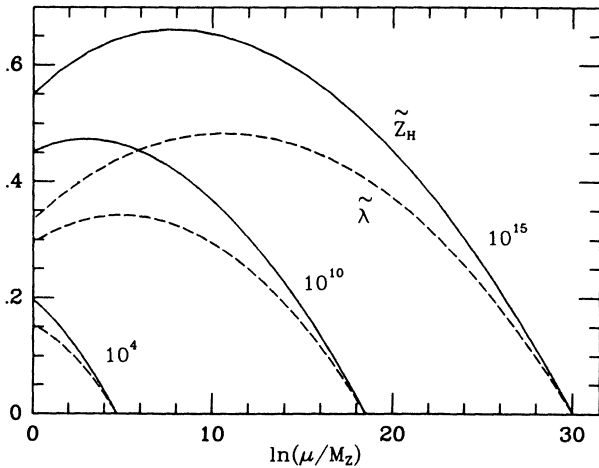


FIG. 4. The renormalization-group evolution of the wave-function normalization constant \tilde{Z}_H (solid lines) and quartic coupling $\tilde{\lambda}$ (dashed lines) for three different scales Λ . Initial values of $\tilde{\lambda}$ are chosen to be precisely on the fixed point. Both quantities go to zero at $\mu=\Lambda$.

$$\begin{aligned} \bar{g}_1^2(M_Z) &= 0.127 \pm 0.009, \\ \bar{g}_2^2(M_Z) &= 0.446 \pm 0.020, \\ \bar{g}_3^2(M_Z) &= 1.44 \pm 0.19. \end{aligned} \quad (4.11)$$

We calculate errors both from the uncertainties of the experimental input and by varying the initial conditions at Λ . For high Λ the uncertainty in $\bar{\alpha}_3(M_Z)$ dominates the error while for Λ the errors become bigger due to the use of perturbation theory. The quoted perturbative errors are obtained by varying the top-quark mass so that $\bar{\alpha}_t = \bar{g}_t^2/4\pi$ becomes unity at the scale Λ , instead of infinity. Further small corrections are expected from higher-order contributions to the fixed points.

The Higgs-boson mass will likewise be determined by the evolution of $\tilde{\lambda}$ given by

$$16\pi^2 \frac{d\tilde{\lambda}}{dt} = 12[\tilde{\lambda}^2 + (\bar{g}_t^2 - A)\tilde{\lambda} + B - \bar{g}_t^4], \quad (4.12)$$

where

$$A = \frac{1}{4}\bar{g}_1^2 + \frac{3}{4}\bar{g}_2^2, \quad B = \frac{1}{16}\bar{g}_1^4 + \frac{1}{8}\bar{g}_2^2\bar{g}_2^2 + \frac{3}{16}\bar{g}_2^4. \quad (4.13)$$

In Fig. 5 we present the results of numerically integrating Eq. (4.12) with the corresponding evolution of \bar{g}_t .

To understand the behavior of the solutions for $\tilde{\lambda}$ it is convenient to define $x = \tilde{\lambda}\bar{g}_t^{-2}$. The compositeness conditions of Eq. (4.3) require that $\tilde{\lambda} = \tilde{\lambda}/\bar{g}_t^4 \rightarrow 0$ as $\mu \rightarrow \Lambda$. Consider Eq. (4.12) with $A \approx B \approx 0$:

$$\begin{aligned} 16\pi^2 \frac{dx}{dt} &= 12\bar{g}_t^2(x^2 + x/4 - 1) \\ &= 12\bar{g}_t^2(x - x_-)(x - x_+), \end{aligned} \quad (4.14)$$

$$x_{\pm} = (-1 \pm \sqrt{65})/8, \quad x_+ \approx 0.88, \quad x_- \approx -1.13. \quad (4.15)$$

Since the right-hand side (RHS) of Eq. (4.14) factorizes

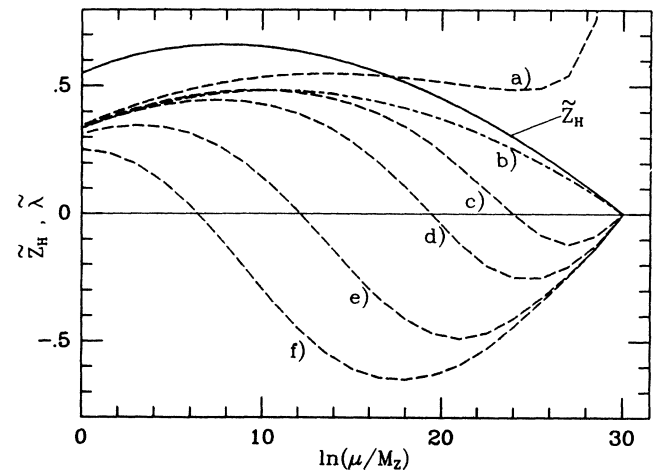


FIG. 5. The evolution of $\tilde{\lambda}$ for different initial values and $\Lambda=10^{15}$ GeV. In (a) the initial value is chosen slightly above the fixed point and $\tilde{\lambda}$ diverges at Λ . In this case the compositeness condition cannot be satisfied. Case (b) corresponds to evolution on the low-energy attractive fixed point. The cases (c)–(f) show that the low-energy result is insensitive to the initial conditions at Λ . \tilde{Z}_H is also plotted as a solid line.

TABLE I. The predictions for the physical top-quark and Higgs-boson mass for different scales Λ . One-loop β functions are used with $g_1^2(M_Z)=0.127\pm 0.009$, $g_2^2(M_Z)=0.446\pm 0.020$, $\alpha_s(M_Z)=0.115\pm 0.015$, and $M_Z=91.17$ GeV as input. The numbers are obtained for the central value of these input data and requiring the on-shell condition $\bar{m}(m)=m$. Variation of the gauge couplings within their errors results to a very good approximation in a change of ± 6 GeV for the top-quark mass and ± 4 GeV for the Higgs-boson mass. The rows labeled "pert." show the change in the result if we change the couplings at the cutoff to unity instead of infinity, as a measure of the errors induced by using perturbation theory.

Λ (GeV)	10^{19}	10^{17}	10^{15}	10^{13}	10^{11}	10^{10}	10^9	10^8	10^7	10^6	10^5	10^4
m_t^{phys} (GeV)	218	223	229	237	248	255	264	277	293	318	360	455
Pert.	± 2	± 3	± 3	± 3	± 5	± 6	± 7	± 9	± 12	± 16	± 25	± 45
m_H^{phys} (GeV)	239	246	256	268	285	296	310	329	354	391	455	605
Pert.	± 3	± 3	± 4	± 5	± 8	± 9	± 11	± 15	± 21	± 32	± 56	± 142

into $\bar{g}_i^2 F(x)$, and \bar{g}_i is diverging as we approach Λ , we can see that the variable $x = \bar{\lambda} \bar{g}_i^{-2}$ grows faster than \bar{g}_i^2 for $x > x_+$. Thus $\bar{\lambda}$ is diverging as it approaches Λ and we cannot satisfy the compositeness conditions on this trajectory. For $x = x_+$ we have an ultraviolet unstable fixed point, and since the β function (4.14) vanishes, x remains constant and therefore $\bar{\lambda} = \bar{g}_i^{-2} x_+$. On the other hand, for $x_- \leq x < x_+$, Eq. (4.14) shows that x is driven toward the fixed-point x_- . In this case $\bar{\lambda}$ evolves as $\bar{g}_i^{-2} x_-$ and will tend to zero as it approaches Λ . The ratio $\bar{\lambda}/\bar{Z}_H$ approaches a constant, indicating that the two quantities do not run independently.

For the physical-Higgs-boson mass we have again two mechanisms which make the prediction very stable. If we start with the compositeness condition at Λ then the preceding discussion shows that the ultraviolet unstable fixed point x_+ becomes attractive as we evolve downwards in scale. This means that $\bar{\lambda}$ is attracted toward $\bar{g}_i^{-2} x_+ = \bar{Z}_H x_+$. Once the couplings become smaller the effect of the smoothly varying gauge couplings is important which further reduces the sensitivity to the precise initial value at Λ . Thus we conclude that the compositeness condition forces the low-energy values close to the infrared-stable fixed point. This corresponds to the dashed lines in Fig. (4) and the dashed-dotted line (b) in Fig. 5. The resulting Higgs-boson masses as a function of Λ are also shown in Table I together with their errors.

B. Phenomenological constraints

The resulting prediction of the full standard-model analysis is a top-quark mass that might be considered large in comparison to certain published theoretical upper limits. Indeed, it has been claimed that the ρ parameter limit implies $m_t \lesssim 180$ to 200 GeV (Ref. 7), and this is the most stringent quoted limit. Our principal comments concerning the ρ parameter limit are as follows.

(i) The quoted limit of Amaldi *et al.* arises from a two-parameter fit to a confidence-level distribution. This confidence-level distribution is derived from comparing the results of a global analysis of neutrino deep-inelastic scattering⁷ (ν DIS) to $\sin^2\theta_W = \pi\alpha/[\sqrt{2}G_F(1 - \Delta R)M_Z^2]$. Here ΔR parametrizes the radiative corrections which bring these two independent determinations into agreement, and is a function of m_t . Other indepen-

dent determinations of $\sin^2\theta_W$ have significantly larger errors, are thus of less statistical weight, and may for the purposes of discussion be ignored presently, though they are included in our figures. Of central importance is the magnitude of the quoted errors of the ν DIS, as we comment upon below in (ii).

The inclusion of the precisely measured value of $M_Z=91.17\pm 0.18$ by the SLAC Linear Collider (SLC) (and now CERN LEP) drastically changes the statistical weight of $\sin^2\theta_W$ as defined through the formulas

$$\sin^2\theta_W \cos^2\theta_W = A^2 / (1 - \Delta R) M_Z^2, \quad A^2 = \frac{\pi\alpha}{\sqrt{2}G_F}. \quad (4.16)$$

Also the CHARM II Collaboration has published a new determination of $\sin^2\theta_W$ for $\nu-e$ (Ref. 8). Inclusion of all these new data leads to Fig. 6 where curve (a) corresponds to the Amaldi *et al.* analysis of neutrino deep-inelastic scattering. The allowed region can be contrasted with Fig. 5 of Ref. 7 prior to the precise measurement of M_Z and is now significantly more restrictive. For our

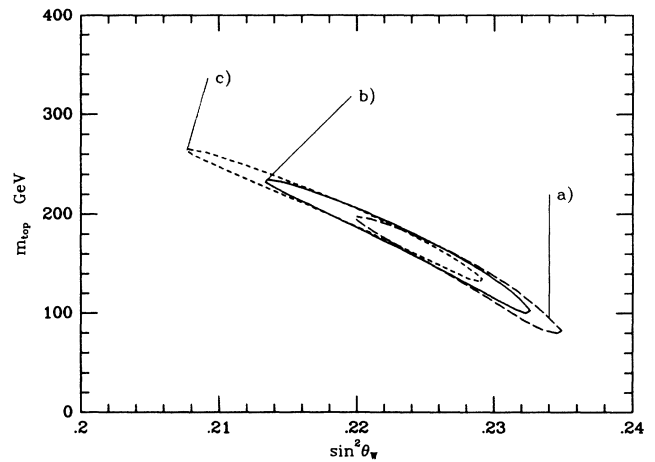


FIG. 6. Allowed regions (at 90% C.L.) for m_t and $\sin^2\theta_W$ for three error hypotheses in the ν DIS experiments. These are drawn for (a) $m_c = 1.5\pm 0.3$ GeV [equivalent to Amaldi *et al.* (Ref. 7) with precise M_Z and $m_H \approx 250$ GeV]; (b) $m_c = 1.3\pm 0.5$ GeV apropos (Ref. 8); (c) disregarding deep-inelastic-scattering data to indicate its overall statistical weight in the limit on m_t .

plot in Fig. 6 we choose $m_H \simeq 260$ GeV as suggested by our model.

(ii) One should understand that the high statistics of all of the ν DIS experiments owes to copious data in the regime where the charm quark is being excited in charged-current processes (particularly the narrow band beam CERN experiments). Yet no description of the charm threshold is perfect below ~ 80 GeV. Other effects, such as hard-gluon radiative corrections, may be significant. We further emphasize here that m_c should be viewed as a parameter in the slow rescaling analysis, and should not be taken literally as the physical charm mass. The meaning of the ascribed error in the parameter $m_c = 1.5 \pm 0.3$ GeV is unclear from the discussion of Ref. 7.

The Chicago-Columbia-Fermilab-Rochester (CCFR) Collaboration⁸ has obtained data at energies in and well above the charm threshold region and future determinations of $\sin^2\theta_W$ from this data may be subject to less uncertainty in the charged-current processes. Their present fit to the parameter m_c is $m_c = 1.31_{-0.48}^{+0.64}$ GeV. For the sake of discussion, taking exclusively the results of Ref. 8 would imply an approximate doubling of the overall ν DIS errors which would drastically reduce its statistical weight as well as shifting the central values, leading to a lower mean $\sin^2\theta_W$. Thus, through the m_t dependence of ΔR (Ref. 9), this would translate into a higher upper limit than derived in Ref. 7.

Simply to give the reader a feeling for this sensitivity to quoted errors, we note that upon replacing $m_c = 1.5 \pm 0.3$ GeV by 1.3 ± 0.5 GeV, the ν DIS data correspond to the increase in the 90% confidence level $m_t \lesssim 200$ to $m_t \lesssim 250$ GeV in Fig. 6. Thus, in Fig. 6 we give the curves (b) representing the confidence-level contours for m_t with the liberalized error assumptions. We also present the determination sans ν DIS in curves (c) to give the reader a feeling for the overall ν DIS statistical weight in deriving the top-quark-mass limit. We emphasize that we do not argue here against the applicability of ν DIS in obtaining a precision test of the standard model, nor that the analysis of Ref. 7 is herein superseded, but rather we wish to emphasize the important sensitivity to the quoted errors and, in turn, to uncertainties in the underlying hadronic processes.

In the left box denoted (A) of Fig. 7 we have displayed several other determinations of $\sin^2\theta_W$ from, e.g., atomic parity violation, νe scattering, etc. The combined results from four deep-inelastic-scattering experiments for two different values of the fitting parameter m_c (1.5 ± 0.3 GeV and 1.3 ± 0.5 GeV) are also shown. The box denoted (B) shows the resulting combined values for the two fitting parameter assumptions. These are then to be compared with box (C). The combined scattering data of the box (B) have a small top-quark-mass dependence which is not displayed here (less than 20% for the indicated range of m_t in the right box). Note the relatively strong dependence of these results on both m_c and its error due to the change of the central value and statistical weight.

In box (C) we show $\sin^2\theta_W$ as obtained from Eq. (4.16) for various values of m_t . The dependence on the top-quark mass arising through ΔR is $\propto m_t^2$ for large m_t ; the

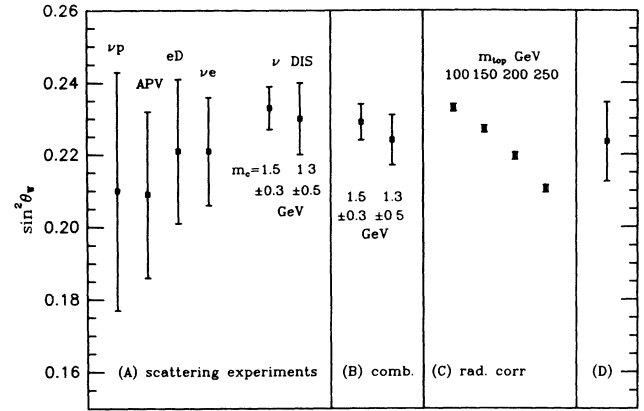


FIG. 7. Comparison of $\sin^2\theta_W$ from different experiments with M_W , M_Z , and radiative corrections. Box (A) shows data from different experiments (the mild radiative corrections for $m_t = 45$ GeV and $m_H = 100$ GeV are included here as in Ref. 8). The lower νe point represents a combination of CHARM and BNL E-734 accounting 80% of the world's data on νe reactions with well-controlled systematic errors [see Abe *et al.* (Ref. 8)]. Box (B) shows the combined result to be compared those displayed in box (C). Box (D) shows $\sin^2\theta_W = 1 - M_W^2/M_Z^2$.

Higgs-boson-mass dependence is very mild and we choose 200 GeV. To the far right in box (D) we give the present experimental value for the definition $\sin^2\theta_W = 1 - M_W^2/M_Z^2$ using the combined results of the UA1, UA2, and Collider Detector at Fermilab (CDF) Collaborations for M_W and M_Z . One can see that, upon comparing to the previous data, the errors here principally in the W mass are too large to lead to a significant top-quark-mass bound, but this situation may change in the not-too-distant future.

Thus, the oft-quoted limit on m_t arises essentially in comparing the ν DIS results of box (B) to the results in box (C) which are sensitive to m_t . The resulting limit hinges crucially upon the experimental errors in ν DIS. We see from Fig. 7 that it does not appear to be in significant conflict with these data to allow m_t/M_Z to be as large as 250 GeV.

In summary, we feel that it is premature to reject predictions of a very heavy top quark, up to at least ~ 250 GeV, based upon the present status of the precision measurements to date. Note that, by incorporating the data with our prediction, we favor $\Lambda \gtrsim 10^{11}$ GeV. The phenomenological predictions for $\sin^2\theta_W$ and M_W are summarized by the equations

$$\sin^2\theta_W = 0.215 \pm 0.002 + 0.00017(230 - m_t), \quad (4.17)$$

$$M_W = 80.73 \pm 0.15 + 0.009(m_t - 230). \quad (4.18)$$

If, ultimately, the theoretical top-quark-mass prediction proves to be too high then it is still possible, albeit possibly less compelling, to maintain this mechanism by assuming that the gap equation (2.2) is saturated by a fourth generation. The top quark then plays no important role itself in the symmetry breaking of the standard model and should have a mass between current lower bounds, but presumably much less than the predictions

TABLE II. Predictions for a degenerate fourth-generation quark doublet with the same input data as in Table I. The top-quark and the fourth-generation leptons are assumed to be much lighter than this quark doublet. The variation of the gauge couplings results in a change of ± 7 GeV for the quark masses and ± 5 GeV for the Higgs-boson mass.

Λ (GeV)	10^{19}	10^{17}	10^{15}	10^{13}	10^{11}	10^{10}	10^9	10^8	10^7	10^6	10^5	10^4
m_t^{phys} (GeV)	199	202	206	212	220	226	233	243	257	277	312	388
Pert.	± 1	± 2	± 2	± 2	± 3	± 4	± 5	± 7	± 10	± 14	± 22	± 39
m_H^{phys} (GeV)	235	241	248	258	272	282	294	310	333	365	423	553
Pert.	± 1	± 2	± 2	± 3	± 4	± 6	± 7	± 10	± 15	± 22	± 39	± 99

for the masses of the fourth generation. In Table II we present the corresponding predictions for the masses of a degenerate fourth doublet. The resulting modified predictions for the Higgs-boson mass as well as the corresponding errors are also shown.

V. CONCLUSIONS

Our principal conclusions are as follows.

(1) The gauged Nambu–Jona-Lasinio mechanism within the framework of the standard model, dynamically broken by a strongly coupled top quark which forms a condensate $\langle \bar{t}t \rangle$, may be implemented in the fermion loop approximation (or large N_c with vanishing g_3). It yields primitive relationships between M_W and m_t and the cutoff Λ , and the Higgs-boson mass is determined as $m_H = 2m_t$. The latter relationship has been emphasized by Nambu.¹ From our point of view, the relationships obtained in this part of the analysis are crude, but correctly indicate that the low-energy effective Lagrangian is the standard model with conventional running of coupling constants and with the special compositeness condition $Z_H \rightarrow 0$ as $\mu \rightarrow \Lambda$.

(2) We infer that $\bar{Z}_H \rightarrow 0$ as $\mu \rightarrow \Lambda$ is the general compositeness condition for the Higgs boson of the full theory. The conventional normalization $Z_H = 1$ implies, equivalently, that \bar{g}_t and $\bar{\lambda}$ diverge as $\mu \rightarrow \Lambda$. This constraint, in turn, implies that the low-energy values of these coupling constants are controlled by the renormalization-group infrared fixed points. Consequently, the low-energy results are insensitive to the detailed behavior of \bar{g}_t and $\bar{\lambda}$ as $\mu \rightarrow \Lambda$.

(3) We give our results for the full standard model as functions of the scale of new physics (or Higgs-boson compositeness scale), λ . Our favored results for m_t are the lower values, as constrained by phenomenological considerations; hence, $m_t \approx 230$ GeV and $m_H \approx 260$ GeV with $\Lambda \approx 10^{15}$ GeV. The mechanism may be adapted to a fourth generation, or a multiple dynamical Higgs-boson scheme, though our primary impetus is in the connection with the top quark since the lower-mass limits on the top quark are suggestive of a strongly coupled system.¹⁰

(4) As per the discussion of Sec. IV B, we believe that existing phenomenological bounds on m_t are not yet sufficiently restrictive to eliminate this scheme for large scales $\Lambda \gtrsim 10^{11}$ GeV and $m_t < 250$ GeV. A better understanding of the ν DIS experiments could possibly rule out our mechanism involving the top-quark dynamics.

As our discussion has indicated, the compositeness of the auxiliary Higgs field leads to predictions for the top-

quark and Higgs-boson masses which are equivalent to effective fixed-point arguments. There is some confusion in the literature on what these fixed points really mean. We emphasize that for us, the fixed point in g_t is that previously considered in Ref. 5, and is quite distinct from that originally proposed by Pendleton and Ross.¹¹ The proposal of Pendleton and Ross focused upon a relationship between g_t and g_3 which causes the ratio of these coupling constants to be fixed for all scales. It is thus a “reduction of coupling constants” in the language of Kubo, Sibold, and Zimmermann.¹² The reduction is really a far-UV constraint; i.e., one assumes that g_t must smoothly go to zero with g_3 ; hence, the rate of change of $\ln g_t/g_3$ must vanish asymptotically. Our mechanism is not a coupling constant reduction in this sense, and g_3 only acts to control g_t as we approach the infrared. Nonetheless, we were driven to consider the infrared fixed point from a specific compositeness condition implemented at Λ . We should remark, however, that with respect to $\bar{\lambda}$, the Higgs-quartic coupling constant, our mechanism does involve, in some sense, a reduction of coupling constants from $\bar{\lambda}$ to \bar{g}_t in the sense of Ref. 12, but here the couplings are diverging together, rather than approaching zero uniformly. Note that previously fixed-point ideas have been used primarily to give probabilistic values of low-energy parameters irrespective of their high-energy values.⁵ We have shown presently that certain renormalization-group trajectories actually follow from compositeness constraints. The derived masses are closely related to the limits obtained from “triviality bounds,” in particular, for a given scale Λ these are equivalent to the simultaneous uppermost allowed values of m_t and m_H (Ref. 13).

Marciano has recently considered ideas that appear somewhat related to those discussed here,¹⁴ but in fact differ substantially in implementation and conclusions. In the first part Marciano reemphasizes the Pendleton-Ross trajectory^{11,12} independently of consideration of dynamical symmetry breaking, and gives improved values using up-to-date input parameters. In the second part of the discussion he considers the Higgs boson to be composite. Here we are in fundamental disagreement on two points. (i) At scales $\mu \ll \Lambda$ the physical Higgs boson, with gauge-invariant kinetic terms, must appear in the effective action, so that effects of its propagation *should be kept in loops*; hence the full standard model with the effects of a pointlike Higgs boson in the renormalization-group equations is relevant. These effects are neglected in Ref. 14. (ii) The compositeness conditions are *boundary conditions* on \bar{g}_t and $\bar{\lambda}$, following from $\bar{Z}_H \rightarrow 0$ as de-

scribed here, and not the asymptotic smoothness assumptions implied in Marciano's work (effectively as in Refs. 11 and 12).

Miransky, Tanabashi, and Yamawaki² have independently proposed the idea of a top-quark condensate driving the breaking of the electroweak interactions, and obtain somewhat different results than those presented here. The authors of Ref. 2 focus upon the idea of large anomalous dimensions for the four-fermion interaction which is interpreted as a signal for dimensional transmutation and the occurrence of a scalar Higgs bound state. We do not share this viewpoint. Indeed, the formation of a *low-mass* scalar state, and top-quark-mass term, is fundamentally tied to the fine-tuning of the gap equation which then leads to the large-distance propagating composite particles. Without this fine-tuning it makes no sense to talk about the scalar-boson state, as then the bubble diagrams produce only a perturbative, local renormalization of the four-fermion interaction. Anomalous dimensions refer only to the local, short-distance renormalization effects, and do not have anything to do with large-distance dynamical propagating fields. For example, in QCD we only consider the short-distance gluon radiative corrections as comprising the anomalous dimension of a given operator, e.g., as in the nonleptonic weak interactions, and which may be arbitrarily large; we do not consider the pion propagation to arise as a consequence of, or play a role in the anomalous dimension. Thus, we believe that there is a confusion in Ref. 2 of short- and long-distance effects and a lack of discussion of the relevant mechanism which leads to long-distance propagating bound states, i.e., the fine-tuning of the gap equation. [We note that this should not be confused with the mechanism of walking technicolor (TC) in which large anomalous dimensions are used justifiably to separate the scales of TC and extended technicolor (ETC).] The vacuum structure of the low-energy theory depends on the fine-tuning of the composite Higgs-boson mass and both symmetric and broken-symmetry phases of the theory can only be understood on the basis of the dynamics of the composite Higgs field. Although our general approaches are similar, it is not clear that the work of Miransky, Tanabashi, and Yamawaki includes the full dynamics of the effective field theory at low energies as required by our analysis. We should further remark that BCS theory has recently been invoked by other authors¹⁵ to conjecture a pattern of quark and lepton masses and mixing angles, an approach that is orthogonal to our attempt to understand dynamical mechanisms of electroweak symmetry breaking.

We have seen that our mechanism favors a large top-quark mass, suggesting a correspondingly large value of $\Lambda \sim 10^{15}$ GeV, and a smaller value of $\sin^2\theta_w \sim 0.21$ to 0.22. These results suggest a number of questions for further analysis, including the possible role of grand unified theories, such as Georgi-Glashow SU(5), where our four-fermion interactions could arise from the high-energy GUT symmetry breaking. Of course, the gap equation solutions for a low-energy electroweak symmetry breaking demands a fine-tuning, equivalent to the usual gauge-hierarchy problem. Perhaps one is led to a supersymmetric version of this discussion [and we remark that in the case of SUSY SU(5) the fixed-point predictions for m_t do not radically change¹⁶]. Or, the nature of the dynamical breaking may be subtle and possibly a new mechanism can be found to solve the fine-tuning problem which locks G into approximate equality with G_c . It seems to be interesting to explore those theories that will provide the effective interaction of Eq. (1.1), which was the starting point for our analysis, with an eye to understanding the origin of the small quark masses and mixing angles.

ACKNOWLEDGMENTS

We wish to thank Professor Y. Nambu for several discussions concerning his work, Dr. R. Bernstein regarding the ρ parameter limits and phenomenology, and Professor J. D. Bjorken and Professor J. Rosner for useful comments.

APPENDIX A: FERMIONIC BUBBLE APPROXIMATION

The present discussion shows how the dynamical-symmetry-breaking mechanism through top-quark condensation works in a fermionic bubble approximation in detail. We presently ignore all gauge-boson and composite-Higgs-boson radiative corrections, keeping only fermion loops.

We first recall the solution to the gap equation for the induced top-quark mass. This is indicated as in Fig. 1 and Eq. (2.1):

$$m_t = -\frac{1}{2}G \langle \bar{t}t \rangle \quad (\text{A1})$$

$$= 2GN_c m_t \frac{i}{(2\pi)^4} \int d^4l (l^2 - m_t^2)^{-1}. \quad (\text{A2})$$

We shall use Eq. (A2) in what follows. The result of evaluating Eq. (A2) with a momentum-space cutoff Λ is as given in Eq. (2.3).

We consider the sum of scalar bubbles of Fig. 2 generated by the interaction Eq. (1.1):

$$\Gamma_s(p^2) = -\frac{1}{2}G - \left(\frac{1}{2}G\right)^2 i \int d^4x e^{ipx} \langle T \bar{t}t(0) \bar{t}t(x) \rangle_{\text{connected}} + \dots \quad (\text{A3})$$

We see that we may formally sum the series to obtain

$$\Gamma_s(p^2) = -\frac{1}{2}G \left[1 - 2GN_c \frac{i}{(2\pi)^4} \int d^4l (l^2 - m_t^2)^{-1} - GN_c (4m_t^2 - p^2) \frac{i}{(2\pi)^4} \int d^4l (l^2 - m_t^2)^{-1} [(p+l)^2 - m_t^2]^{-1} \right]^{-1}. \quad (\text{A4})$$

Here the second and third terms in the denominator of Eq. (A4) come from a rearrangement of the terms in the numerator of the Feynman loop integral and a shift of the loop momentum for the fermions. We thus see that the first two terms in the denominator of Eq. (A4) cancel by virtue of the gap equation (A2). Thus, performing the loop integrations we arrive at

$$\Gamma_s(p^2) = -\frac{1}{2N_c} \left[(4m_t^2 - p^2)(4\pi)^{-2} \int_0^1 dx \ln \{ \Lambda^2 / [m_t^2 - x(1-x)p^2] \} \right]^{-1}. \quad (\text{A5})$$

Analogously we obtain the results of Eqs. (2.7) and (2.9).

Turning to the W -boson vacuum polarization, we have

$$\frac{1}{g_2^2} D_{\mu\nu}^W(p)^{-1} = \frac{1}{g_2^2} (p^\mu p^\nu - g^{\mu\nu} p^2) + \frac{i}{2} \int d^4x \langle T \bar{t}_L \gamma_\mu b_L(0) \bar{b}_L \gamma_\nu t_L(x) \rangle, \quad (\text{A6})$$

where g_2 is the SU(2) coupling constant. For the T -ordered product we again expand in the interaction Lagrangian of Eq. (1.1) and sum the planar bubbles, Fig. 3. We assume the top quark has a mass satisfying Eq. (2.3), and the gap equation is satisfied in the loop expansion, which maintains the gauge invariance. Notice that this sum can thus be written in terms of the flavor bubbles evaluated in Eq. (2.10):

$$\begin{aligned} \frac{1}{g_2^2} D_{\mu\nu}^W(p)^{-1} &= \frac{1}{g_2^2} (p^\mu p^\nu - g^{\mu\nu} p^2) + \frac{1}{4} \frac{i}{(2\pi)^4} \int d^4p \text{Tr}[\gamma_\mu (1 - \gamma_5)(\not{p} + \not{k})^{-1} \gamma_\nu (1 - \gamma_5)(\not{p} + \not{k} - m_t)^{-1}] \\ &\quad - \frac{1}{8} \Gamma_F(p^2) \frac{i}{(2\pi)^4} \int d^4l \text{Tr}[\gamma_\mu (1 - \gamma_5)(\not{p} + \not{l})^{-1} (1 + \gamma_5)(\not{l} - m_t)^{-1}] \\ &\quad \times \frac{i}{(2\pi)^4} \int d^4q \text{Tr}[\gamma_\nu (1 - \gamma_5)(\not{p} + \not{q})^{-1} (1 + \gamma_5)(\not{q} - m_t)^{-1}]. \end{aligned} \quad (\text{A7})$$

An evaluation of these expressions leads to

$$\begin{aligned} \frac{1}{g_2^2} D_{\mu\nu}^W(p)^{-1} &= (p^\mu p^\nu / p^2 - g^{\mu\nu}) \left[\frac{1}{g_2^2} p^2 + p^2 N_c (4\pi)^{-2} \int_0^1 dx 2x(1-x) \ln \{ \Lambda^2 / [(1-x)m_t^2 - x(1-x)p^2] \} \right. \\ &\quad \left. - m_t^2 N_c (4\pi)^{-2} \int_0^1 dx (1-x) \ln \{ \Lambda^2 / [(1-x)m_t^2 - x(1-x)p^2] \} \right]. \end{aligned} \quad (\text{A8})$$

We see that the overall inverse propagator is transverse, corresponding to a gauge-invariant Higgs mechanism. Nonetheless there is a zero for nontrivial momentum, corresponding to the induced W -boson mass. From these follow Eq. (2.11) to Eq. (2.16).

Analogous results are obtained for the neutral-gauge-boson masses. Presently we consider the inverse propagator of the neutral gauge bosons as a 2×2 matrix of the form

$$\frac{1}{g_i g_j} D_{\mu\nu}^0(p)^{-1} = \begin{bmatrix} 1/g_2^2 & 0 \\ 0 & 1/g_1^2 \end{bmatrix} (p^\mu p^\nu - g^{\mu\nu} p^2) + \frac{1}{2} i \int d^4x \begin{bmatrix} \langle T j_\mu^3(0) j_\nu^3(x) \rangle & \langle T j_\mu^3(0) j_\nu^0(x) \rangle \\ \langle T j_\mu^0(0) j_\nu^3(x) \rangle & \langle T j_\mu^0(0) j_\nu^0(x) \rangle \end{bmatrix}, \quad (\text{A9})$$

where g_1 is the U(1) coupling constant. Here the currents are the usual SU(2) and U(1) neutral currents in the unmixed basis,

$$j_\mu^3 = \bar{t}_L \gamma_\mu t_L - \bar{b}_L \gamma_\mu b_L, \quad (\text{A10})$$

$$j_\mu^0 = \frac{1}{3} (\bar{t}_L \gamma_\mu t_L + \bar{b}_L \gamma_\mu b_L) + \frac{4}{3} (\bar{t}_R \gamma_\mu t_R) - \frac{2}{3} (\bar{b}_R \gamma_\mu b_R), \quad (\text{A11})$$

and the numerical factors in the individual terms of j_μ^0 are the U(1) weak hypercharges. Again we expand in the interaction Lagrangian of Eq. (1.1) and sum the planar bubbles, Fig. 3. This can be evaluated to yield

$$\frac{1}{g_i g_j} D_{\mu\nu}^0(p)^{-1} = (p^\mu p^\nu / p^2 - g^{\mu\nu}) \left[\begin{bmatrix} 1/g_2^2(p^2) & 0 \\ 0 & 1/g_1^2(p^2) \end{bmatrix} p^2 - \begin{bmatrix} 1 & -1 \\ -1 & 1 \end{bmatrix} f^2(p^2) \right], \quad (\text{A12})$$

where

$$\frac{1}{g_2^2(p^2)} = \frac{1}{g_2^2} + \frac{1}{2} (4\pi)^{-2} \int_0^1 dx 2x(1-x) \left[\frac{4}{3} N_c \ln \{ \Lambda^2 / [m_t^2 - x(1-x)p^2] \} + \frac{2}{3} N_c \ln \{ \Lambda^2 / [m_b^2 - x(1-x)p^2] \} \right] \quad (\text{A13})$$

and

$$\frac{1}{g_1^2(p^2)} = \frac{1}{g_1^2} + \frac{1}{2} (4\pi)^{-2} \int_0^1 dx 2x(1-x) \left(\frac{20}{9} N_c \ln \{ \Lambda^2 / [m_t^2 - x(1-x)p^2] \} + \frac{2}{9} N_c \ln \{ \Lambda^2 / [m_b^2 - x(1-x)p^2] \} \right) \quad (\text{A14})$$

and we include, for completeness,

$$\frac{1}{\bar{g}_2^2(p^2)} = \frac{1}{g_2^2} + N_c(4\pi)^{-2} \int_0^1 dx \, 2x(1-x) \ln\{\Lambda^2/[xm_b^2 + (1-x)m_t^2 - x(1-x)p^2]\} . \quad (\text{A15})$$

Finally,

$$\begin{aligned} f^2(p^2) = & \frac{1}{6}N_c(4\pi)^{-2} \int_0^1 dx \, 2x(1-x)p^2 \ln\left\{\frac{m_b^2 - x(1-x)p^2}{m_t^2 - x(1-x)p^2}\right\} + \frac{1}{2}N_c m_t^2(4\pi)^{-2} \int_0^1 dx \, \ln\{\Lambda^2/[m_t^2 - x(1-x)p^2]\} \\ & + \frac{1}{2}N_c m_b^2(4\pi)^{-2} \int_0^1 dx \, \ln\{\Lambda^2/[m_b^2 - x(1-x)p^2]\} \end{aligned} \quad (\text{A16})$$

and

$$\begin{aligned} \bar{f}^2(p^2) = & N_c(4\pi)^{-2} \int_0^1 dx \, [xm_b^2 + (1-x)m_t^2] \\ & \times \ln\{\Lambda^2/[xm_b^2 + (1-x)m_t^2 - x(1-x)p^2]\} . \end{aligned} \quad (\text{A17})$$

Note that $f(p^2)$ [$\bar{f}(p^2)$] may be interpreted as the decay constant of the neutral [charged] Goldstone mode.

APPENDIX B: RENORMALIZATION OF GAUGE COUPLING CONSTANTS

We thus see that the gauge couplings are subject to logarithmic evolution between the scales Λ and M_W . We may write the low-energy gauge coupling constants from Eqs. (A13) and (A14):

$$\frac{1}{g_2^2(0)} = \frac{1}{g_2^2} + \frac{1}{6}N_c(4\pi)^{-2} \left[\frac{4}{3} \ln(\Lambda^2/m_t^2) + \frac{2}{3} \ln(\Lambda^2/m_b^2) \right] \quad (\text{B1})$$

and

$$\frac{1}{g_1^2(0)} = \frac{1}{g_1^2} + \frac{1}{6}N_c(4\pi)^{-2} \left[\frac{20}{9} \ln(\Lambda^2/m_t^2) + \frac{2}{9} \ln(\Lambda^2/m_b^2) \right] . \quad (\text{B2})$$

We also have the running of \bar{g}_2 from the W -boson propagator, Eq. (2.14):

$$\begin{aligned} \frac{1}{\bar{g}_2^2(0)} = & \frac{1}{g_2^2} + N_c(4\pi)^{-2} \int_0^1 dx \, 2x(1-x) \\ & \times \ln\{\Lambda^2/[xm_b^2 + (1-x)m_t^2]\} . \end{aligned} \quad (\text{B3})$$

We see that the *high-energy* renormalization-group running of g_2 and \bar{g}_2 implied by the net coefficients of the $\ln\Lambda$ in Eqs. (B3) and (A13) is identical. Thus the high-energy running in the unbroken phase corresponding to momenta $p^2 \gg m_t^2$ will be consistently that given by either of Eq. (B3) or Eq. (A13) for a single SU(2) gauge coupling constant. Moreover, the high-energy running of g_2 is consistent with a single-generation quark-doublet contribution to the usual β function:

$$16\pi^2 \frac{\partial}{\partial \ln\mu} g_2^2 = \left[-\frac{22}{3} + \frac{N_c}{3} n_q + \frac{1}{3} n_l \right] g_2^3 , \quad (\text{B4})$$

where $n_q(n_l)$ is the number of quark (lepton) doublets. Thus, the coefficient of $\ln\Lambda$ in Eq. (B3) or Eq. (A13) corresponds to $n_q = 1$ in the second term on the RHS of Eq. (B4).

Similarly, the high-energy running of g_1 may be read off from Eq. (B2) and again is consistent with a single quark doublet contribution to the usual renormalization-group equation:

$$16\pi^2 \frac{\partial}{\partial \ln\mu} g_1 = \left(\frac{11}{27} N_c n_q + n_l \right) g_1^3 . \quad (\text{B5})$$

The fact that this is just the normal renormalization-group running of these coupling constants from the single isodoublet of quarks in the standard model (neglecting all other contributions, such as gauge-boson loops) indicates that the low-energy effective Lagrangian at this order is just the standard model.

The further renormalization effects below the scale m_t are radiative corrections that show up at low energy, e.g., neutrino scattering for $Q^2 \ll M_W^2$. These involve, essentially, the extrapolation from the on-shell W and Z masses to the low energy measured $\sin^2\theta_W$ and G_F . Does the model lead to new effects here?

We see that

$$f^2(0) = \frac{1}{2}N_c(4\pi)^{-2} [m_t^2 \ln(\Lambda^2/m_t^2) + m_b^2 \ln(\Lambda^2/m_b^2)] \quad (\text{B6})$$

and

$$\begin{aligned} \bar{f}^2(0) = & N_c(4\pi)^{-2} \int_0^1 dx \, [xm_b^2 + (1-x)m_t^2] \\ & \times \ln\{\Lambda^2/[xm_b^2 + (1-x)m_t^2]\} \\ = & f^2(0) + \frac{N_c}{4}(4\pi)^{-2} \left[m_t^2 + m_b^2 \right. \\ & \left. - \frac{2m_t^2 m_b^2}{m_b^2 - m_t^2} \ln(m_b^2/m_t^2) \right] . \end{aligned} \quad (\text{B7})$$

The difference, $\bar{f}^2(0) - f^2(0)$ is essentially the usual correction to the ρ parameter due to weak isospin breaking effects and arises as a radiative correction to many physical processes. There are thus no additional corrections associated with the dynamical-symmetry-breaking mechanism beyond the usual standard-model results. This is analogous to well-known results of Carter and Pagels¹⁷ for other dynamical-symmetry-breaking schemes such as technicolor.

- ¹Y. Nambu, in *New Theories in Physics*, proceedings of the XI International Symposium on Elementary Particle Physics, Kazimierz, Poland, 1988, edited by Z. Ajduk, S. Pokorski, and A. Trautman (World Scientific, Singapore, 1989); a version of this work appears in *New Trends in Strong Coupling Gauge Theories*, 1988 International Workshop, Nagoya-Japan, edited by M. Bando, T. Muta, and K. Yamawaki (World Scientific, Singapore, 1989); and EFI Report No. 89-08, 1989 (unpublished).
- ²V. A. Miransky, M. Tanabashi, and K. Yamawaki, *Mod. Phys. Lett. A* **4**, 1043 (1989); *Phys. Lett. B* **221**, 177 (1989).
- ³Y. Nambu and G. Jona-Lasinio, *Phys. Rev.* **122**, 345 (1961); W. A. Bardeen, C. N. Leung, and S. T. Love, *Phys. Rev. Lett.* **56**, 1230 (1986); Report No. FERMILAB-Pub-89/22-T (unpublished).
- ⁴J. D. Bjorken, *Ann. Phys. (N.Y.)* **24**, 174 (1963); T. Eguchi, *Phys. Rev. D* **14**, 2755 (1976); F. Cooper, G. Guralnik, and N. Snyderman, *Phys. Rev. Lett.* **40**, 1620 (1978).
- ⁵C. T. Hill, *Phys. Rev. D* **24**, 691 (1981); C. T. Hill, C. N. Leung, and S. Rao, *Nucl. Phys.* **B262**, 517 (1985).
- ⁶I. Montvay, in *Proceedings of the International Europhysics Conference on High Energy Physics*, Uppsala, Sweden, 1987, edited by O. Botner (European Physical Society, Geneva, Switzerland, 1987); J. Shigemitsu, *Phys. Lett. B* **226**, 364 (1989); **189**, 164 (1987).
- ⁷U. Amaldi *et al.*, *Phys. Rev. D* **36**, 1385 (1987); with slightly more restrictive assumptions, see also G. Costa *et al.*, *Nucl. Phys.* **B297**, 244 (1988).
- ⁸R. Brock, in *Proceedings of the Conference on New Directions in Neutrino Physics at Fermilab*, Batavia, Illinois, 1988, edited by R. Bernstein (unpublished); R. Bernstein and G. P. Yeh (private communications). For a recent study by the CCFR Collaboration of the slow rescaling parametrization favoring $m_c = 1.3 \pm 0.5$ GeV, see C. Foudas *et al.* (unpublished). The ν_e result follows from the recent analysis of K. Abe *et al.*, *Phys. Rev. Lett.* **62**, 1709 (1989).
- ⁹A. Sirlin, *Phys. Rev. D* **22**, 971 (1980); W. Marciano and A. Sirlin, *ibid.* **22**, 2695 (1980); **29**, 945 (1984); D. Yu. Bardin, S. Riemann, and T. Riemann, *Z. Phys. C* **32**, 121 (1986); F. Jegerlehner, *ibid.* **32**, 425 (1986).
- ¹⁰P. Langacker, W. Marciano, and A. Sirlin, *Phys. Rev. D* **36**, 2191 (1987).
- ¹¹B. Pendleton and G. G. Ross, *Phys. Lett.* **98B**, 291 (1981).
- ¹²J. Kubo, K. Sibold, and W. Zimmermann, *Phys. Lett. B* **220**, 191 (1989); *Nucl. Phys.* **B259**, 331 (1985).
- ¹³L. Maiani, G. Parisi, and R. Petronzio, *Nucl. Phys.* **B136**, 115 (1978); N. Cabibbo *et al.*, *ibid.* **B158**, 295 (1979); R. Dashen and H. Neuberger, *Phys. Rev. Lett.* **50**, 1847 (1983); D. J. E. Callaway, *Nucl. Phys.* **B233**, 189 (1984); M. Lindner, *Z. Phys. C* **31**, 295 (1986).
- ¹⁴W. J. Marciano, *Phys. Rev. Lett.* **62**, 2793 (1989).
- ¹⁵P. Kaus and S. Meshkov, *Mod. Phys. Lett. A* **3**, 1251 (1988); **4**, 603(E) (1989); H. Fritzsch, in *Flavor Mixing in Weak Interactions*, proceedings of the Europhysics Topical Conference, Erice, Italy, 1984, edited by L.-L. Chau (Ettore Majorana International Science Series, Physical Sciences, Vol. 20) (Plenum, New York, 1984); Munich Report No. MPI-PAE/PTH 22/88 (unpublished); Proceedings of the 60th Birthday Symposium for M. Gell-Mann, Pasadena, California (unpublished).
- ¹⁶J. Bagger, S. Dimopoulos, and E. Masso, *Phys. Rev. Lett.* **55**, 1450 (1985); **55**, 920 (1985); *Phys. Lett.* **156B**, 357 (1985).
- ¹⁷A. Carter and H. Pagels, *Phys. Rev. Lett.* **43**, 1845 (1979).